Final Technical Report on DOE Junior Faculty Development Award

Title: Fundamental Studies of FRC Turbulence

PI: Tobin Munsat, University of Colorado

Grant #: DE-FG02-05ER54841

Colorado FRC Facility Construction – Over the course of this project we developed and contstructed the Colorado FRC facility, which included a custom vacuum vessel, high voltage and firing circuitry, two plasma gun electrodes, and pumping system, and several diagnostics, listed below.

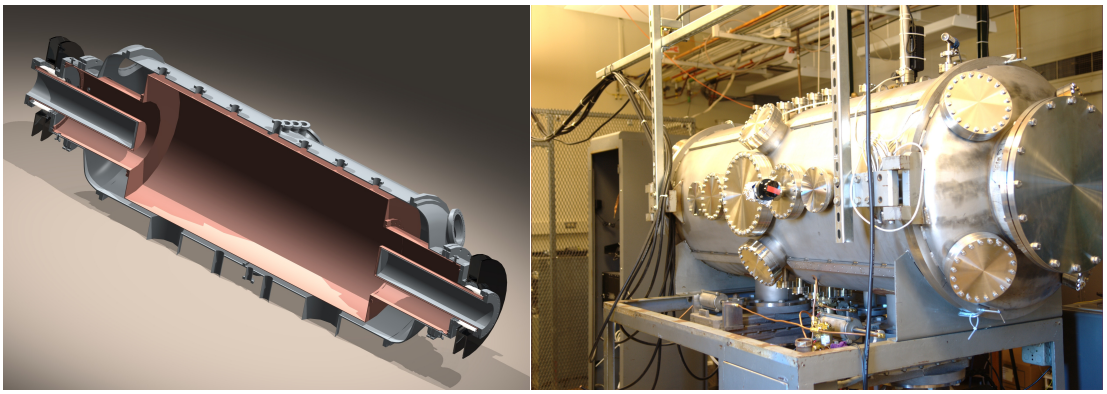

Figure 1. Vacuum vessel CAD and photo.

Diagnostic Development: Laser Interferometer – Density measurements were made with a multichannel CO_2 (10.6 μm) laser interferometer, pictured below. In this system, the primary signal is frequency-downconverted using a 40 MHz acousto-optic modulator, and the intermediate frequency signal is analyzed with a quadrature-detection system to allow for absolute phase recovery.

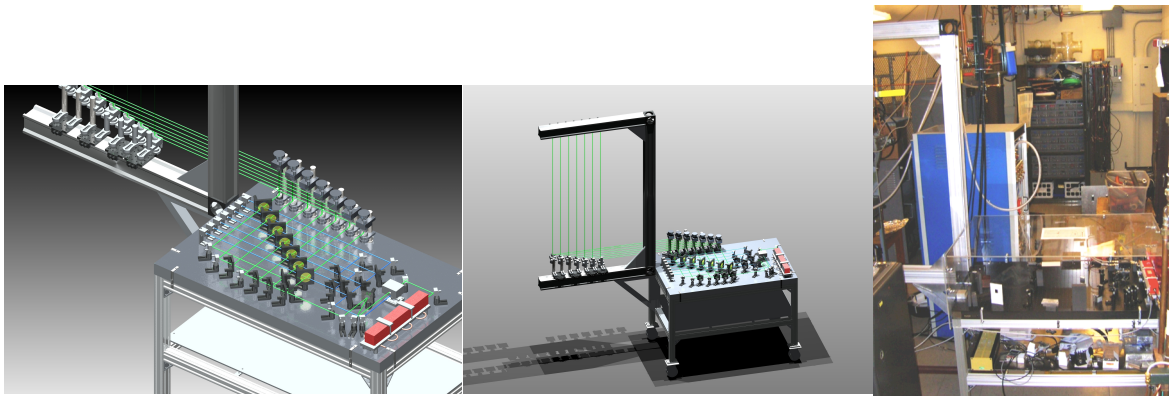

Figure 2. CO_2 Interferometer CAD and photo.

Diagnostic Development; High-Resolution Magnetic Probe Array – We also developed and a high-resolution magnetic probe array for 3-axis measurements of magnetic fluctuations. The array is composed of 16 sets of 3 pickup loops each (x,y,z), arranged into a linear array. Part of this effort is a 48-channel amplifier/integrator set, and the signals are recorded with 40 Msamp/sec waveform recorders for studies of high-frequency magnetic fluctuations.

Diagnostic Development; Triple Probe – We constructed and implemented a triple Langmuir probe for making time-resolved measurements of plasma density, potential, and temperature. This probe was mounted on a movable stalk to enable radial scans (one location per shot).

Physics Results: FRC Formation – By calculating the time history of the gun eigenvalue, we observed indications that the Taylor formation paradigm applies. Figure 3 shows the calculated value of $\lambda(t) = \mu_0 I_{gun}(t)/\Phi_{gun}$, assuming that all of the flux generated by the stuffing magnet links the two electrodes. The dashed horizontal line represents the threshold gun value, $\lambda_c = 20.1\ m^{-1}$. The dotted horizontal line represents the threshold value calculated for the chamber outside the gun, $\lambda_w = 10.2\ m^{-1}$. Dashed and dotted vertical lines indicate where $\lambda(t)$ exceeds each threshold as it increases in time. The time axis of the density (b) is shifted by the propagation time calculated above, so that increases in density may be tentatively identified with a λ value at the time of launch. There is a reasonable match between the identified threshold crossings and increases in the line-integrated density.

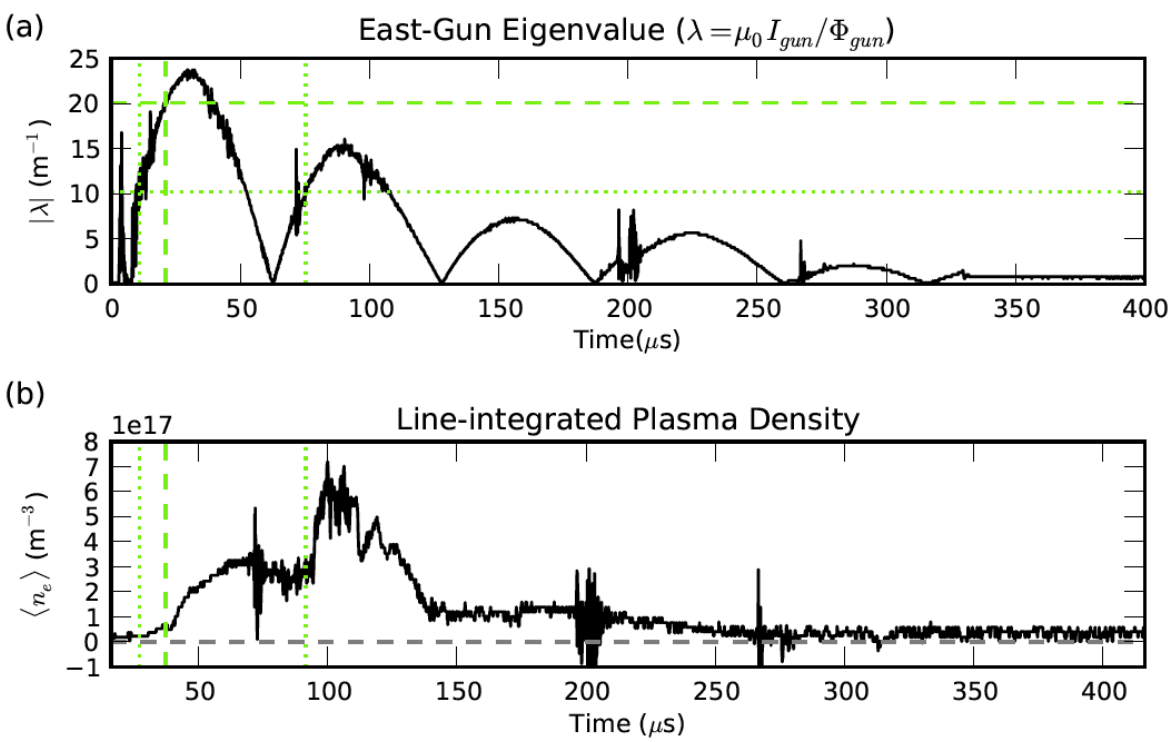

Figure 3. Comparison of spheromak launch threshold with plasma density. (a) Calculated spheromak eigenvalue, λ(t). (b) Line-integrated density, shifted by the propagation time. Density increases coincide with eigenvalue threshold crossings..

During merged operation (firing both guns), there is a marked density increase in most shots that we do not see during single-gun discharges. Figure 4 shows this behavior along with the concurrent λ value for one gun. The single shot magnetic data most easily interpreted in the FRC-merging model is shown in Figure 5, along with the λ traces for both guns (without simultaneous density measurement. It is possible that the behavior of the magnetic field direction near t = 150 μs indicates the formation of an FRC-like object. The azimuthal field decays as the axial field increases. This corresponds to a decay in the toroidal field of a (non-tilted) spheromak in the chamber and an increase the poloidal field of a (non-tilted) FRC. For completeness, plots of the spatio-temporal projections of B (as above) are shown in Figure 6.

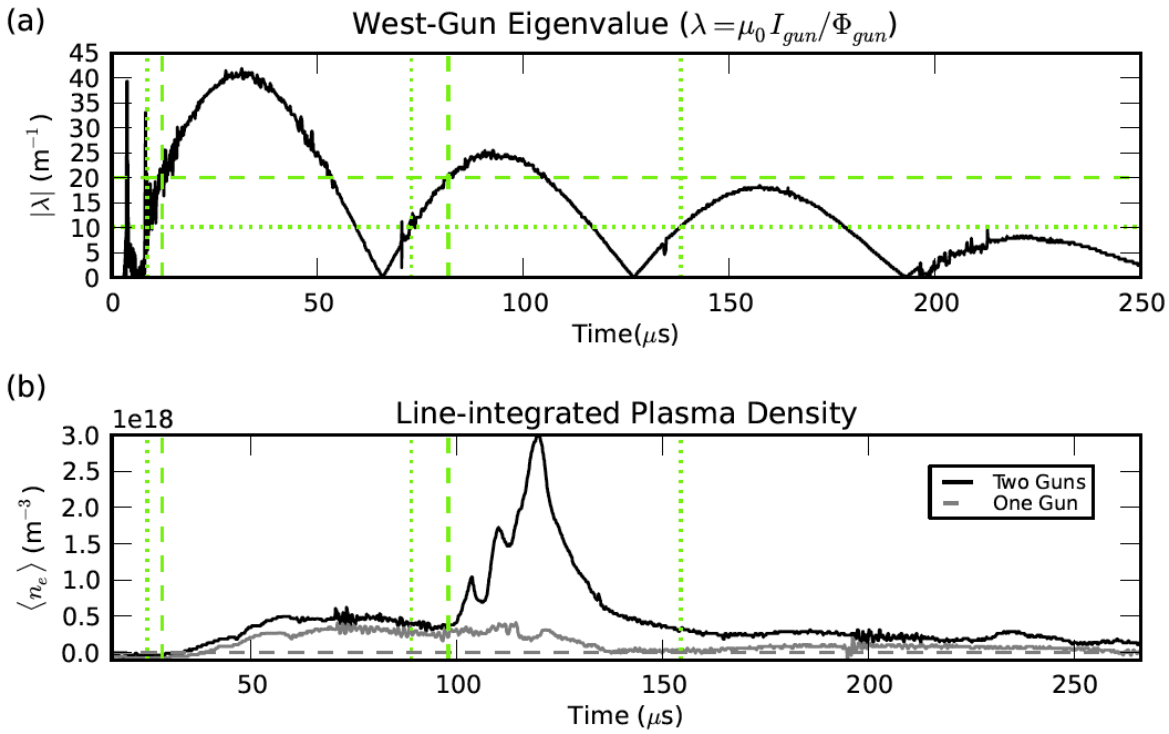

Figure 4. Evolution of line-average density for two-gun discharge (merged). (a) Time evolution of λ for west gun. (b) Time evolution of line-integrated plasma density. A trace for a single-gun discharge using the same gun parameters is shown for contrast in light gray.

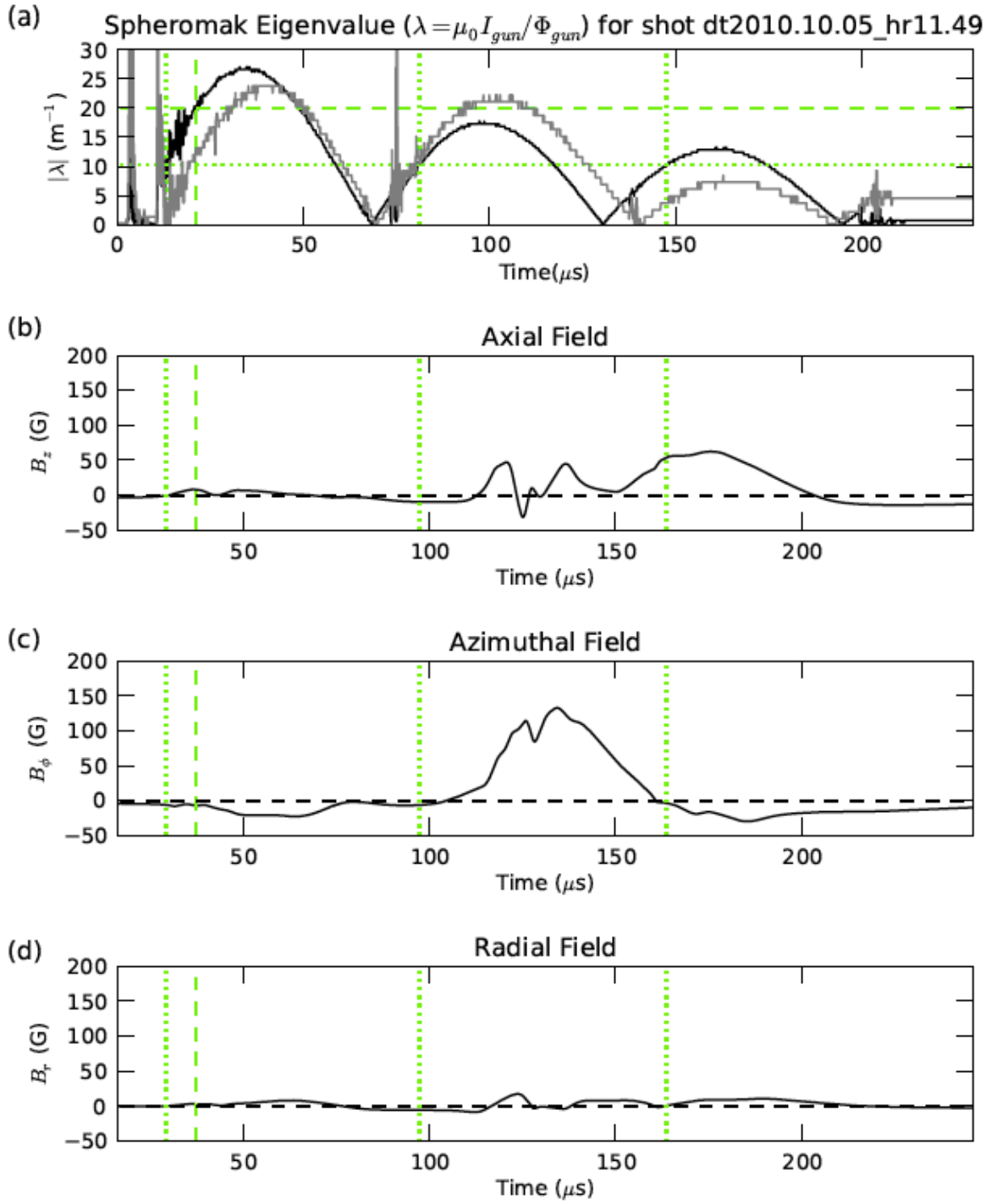

Figure 5. Magnetic traces in the midplane for r = 27.4 cm. The lighter (gray) trace in (a) shows the λ value for the second gun. In the time period shortly after t = 150 μs axial field (b) increases while the azimuthal field (c) decays, indicating an FRC-like object with zero toroidal (azimuthal field) but finite poloidal (radial/axial) field.

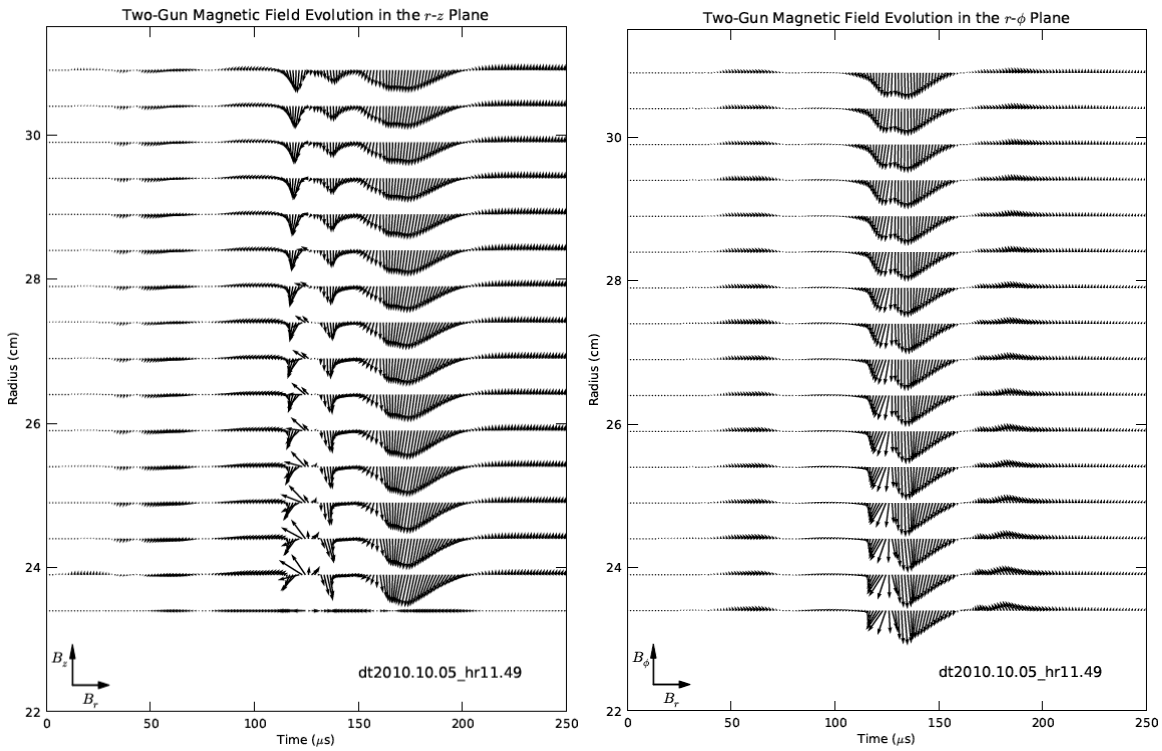

Figure 6. (a) Projection of magnetic field in the r-z plane as a function of time and radius. The rotation of B near t = 125 μs varies strongly along the probe. Both the radial variation and the fast temporal scale for the motion suggest that a localized magnetic structure is passing by the probe. The increase in B_z after t = 150 μs may indicate the formation of a merged object. (b) Projection of magnetic field in the r-phi plane as a function of time and radius. The change in B_r near t = 125 μs is again visible, but B_{phi} is more or less uniform in radius. The strong reduction of B_{phi} just after t = 150 μs may indicate annihilation of toroidal field.

Physics Results: Wave Dispersion Measurements – One of the major goals of Colorado FRC was to estimate the spectral characteristics of fluctuations in an FRC. For this, we developed a technique to extract the relevant spectral information using data from the high-resolution multi-point magnetic probe. Our approach was based on the extensive work by E.J. Powers and colleagues in the 1980s, modified to extract cross-spectral information from non-time-stationary fluctuations by using channel-averaging (taking advantage of the multiple channel-pairs in the magnetic probe) instead of time-block-averaging (used in a two-point measurement). Using this approach, we derive the full two-dimensional distribution of spectral power in frequency and wavenumber space, (not just the power and mean wavenumber versus frequency).

An interesting example of this class of analysis is shown in Fig. 7. Clearly observable in the spectral power map, signatures of spectral power at approximate multiples of a frequency in the ion-cyclotron range suggests that the fluctuations are associated with ion cyclotron harmonics. Ion Berstein waves and ion-cyclotron-harmonic waves have both been discussed in the context of reconnection and particle heating. In cases where we form a merged object, we might expect either or both of these waves to be driven by the merging process.

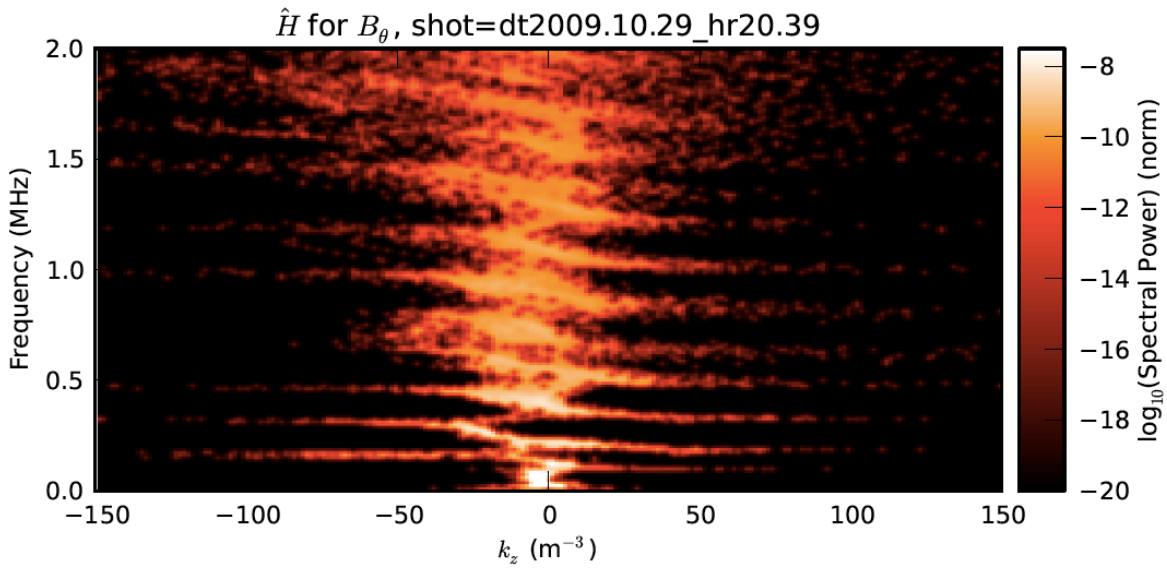

Figure 7. Spectral intensity plot demonstrating fluctuations suggestive of ion-cyclotron-harmonic or ion Bernstein waves.

Student Involvement – Sam Wurzel, the first graduate student on this project, graduated with a Masters degree from the University of Colorado. Jeremy Nuger performed a shorter-term project to develop the high-resolution magnetic probe array. Adam Light, performed part of his PhD work on this project. Additionally, several undergraduate students did honors projects or other research projects on this experiment: William Willcockson (who went on to graduate school at the University of Washington), Leland Ellison (who went on to graduate school at Princeton University), and NUF students Enrique Merino, Onnie Luk, and Drew Cardwell.

Refereed Journal Publications –

The Colorado FRC Experiment, T. Munsat, C.L. Ellison, A. Light, J. Nuger, W. Willcockson, and S. Wurzel, Journal of Fusion Energy **27** (2008).

Conference Presentations and Refereed Publications –

The Colorado FRC Experiment, T. Munsat, C.L. Ellison, A. Light, J. Nuger, W. Willcockson, and S. Wurzel, presented at the ICC 2007 Workshop, College Park MD (2007).

Diagnostic Systems on the Colorado FRC Experiment, S. Wurzel, D. Cardwell, C.L. Ellison, W. Handley, E. Merino, T. Munsat, and W. Willcockson, presented at the 48th APS-DPP Meeting, Philadelphia (2006).

The Colorado FRC Experiment, T. Munsat, D. Cardwell, C.L. Ellison, W. Handley, E. Merino, W. Willcockson, and S. Wurzel, presented at the 48th APS-DPP Meeting, Philadelphia (2006).